POLITECNICO DI TORINO
Repository ISTITUZIONALE

Recycling and reuse of ceramic materials from components of waste solid oxide cells (SOCs)

Original
Recycling and reuse of ceramic materials from components of waste solid oxide cells (SOCs) / Saffirio, S., Anelli, S., Pylypko, S., Rath, M.K., Smeacetto, F., Fiorilli, S.. - In: CERAMICS INTERNATIONAL. - ISSN 0272-8842. - 50:18, Part B(2024), pp. 34472-34477. [10.1016/j.ceramint.2024.06.206]

Availability:
This version is available at: 11583/2990505 since: 2024-07-08T13:34:02Z

Publisher:
Elsevier

Published
DOI:10.1016/j.ceramint.2024.06.206

Terms of use:

This article is made available under terms and conditions as specified in the corresponding bibliographic description in the repository

Publisher copyright

(Article begins on next page)

29 November 2026

Ceramics International 50 (2024) 34472–34477

Contents lists available at ScienceDirect

Ceramics International

journal homepage: www.elsevier.com/locate/ceramint

Short communication

Recycling and reuse of ceramic materials from components of waste solid oxide cells (SOCs)

Sofia Saffirio [a], Simone Anelli [a], Sergii Pylypko [b], Manasa Kumar Rath [b], Federico Smeacetto [a], Sonia Fiorilli [a,*]

[a] Department of Applied Science and Technology, Politecnico di Torino, C.so Duca Degli Abruzzi 24, 10129, Torino, Italy
[b] Elcogen, Valukoja 23, 11415, Tallinn, Estonia

ARTICLE INFO

Handling Editor: P. Vincenzini

Keywords:
Waste SOCs
Recycled ceramics
Critical raw materials
Tape-casting

ABSTRACT

As one of the main waste streams of the manufacturing process of solid oxide cells (SOCs), scrap half-cells - discarded before the deposition of the barrier layer and the air electrode - imply the loss of significant quantities of ceramic composite material containing critical and hazardous elements, namely yttria-stabilized zirconia (YSZ) and NiO. These materials represent more than 90 wt% of an entire anode-supported cell. In this contribution, scrap half-cells were fragmented and subjected to three subsequent milling and sieving (below 25 μm) steps to recover composite NiO-YSZ powders with the appropriate specifications for reuse in SOC manufacturing. The overall characterization in terms of specific surface area, particle size distribution and crystalline phase retention confirmed the suitability of the recovered powders. Half-cells were manufactured including 30 wt% of recovered NiO-YSZ composite powders in their fuel electrode support, produced via tape-casting in combination with 70 wt% of virgin materials. The obtained cells were morphologically, mechanically and electrochemically tested and compared against standard cells constituted by 100 wt% of virgin materials. The electrochemical characterization highlighted 0.68 A cm^{-2} for the standard and recycled cells, at 600 °C and 0.7 V, while at 650 °C and same voltage both cells measured 1.12 A cm^{-2}. This demonstrates the feasibility of recovering scrap SOCs through the presented method.

1. Introduction

In the manufacturing process of solid oxide cells (SOCs), tape-cast and screen-printed components (i.e., NiO fuel contact layer, NiO-3YSZ fuel support layer, NiO-8YSZ fuel functional layer and 8YSZ electrolyte) showing structural defects are discarded before the deposition of the barrier layer and the air electrode. These scrap half-cells derived from manufacturing constitute one of the main waste streams of the SOC production process. As the demand for raw materials for SOC manufacturing is expected to remarkably increase shortly [1], the recovery of critical phases from scrap cells and the reuse for new manufacturing cycles are crucial to target large-scale production and promote circularity in the field of SOC technologies. As reported by S. Sarner et al., a very limited number of studies in the existing literature focus on the recycling of components from SOCs [2]. However, the awareness of the scientific community and policymakers regarding the strategic role of recycling critical materials has been increasingly consolidated. Within this perspective, the authors demonstrated in a previous work the selective separation and recovery of Ni and YSZ from the composite Ni-YSZ composite, derived from the fuel support layer, the fuel functional layer and the electrolyte of operated and dismantled EoL-SOCs. The recovery was achieved by combining hydrothermal treatment and acid-assisted extraction after mechanically removing the air electrode [3]. A similar approach was soon after investigated by Yenesew et al. [4]. Alternative approaches have been proposed by Sarner et al., who reported the re-oxidation of EoL cells and the recovery of NiO-YSZ composite powders after removing the air electrode by acid leaching [5]. A recent work by Kaiser et al. successfully explored the removal of the air electrode through ultrasonic decoating aiming at reducing the manual operation and the use of hazardous chemicals [6].

Here the authors report an effective and straightforward strategy to recover discarded half-cells. Through the presented method, NiO-YSZ composite powders retrieved after cell milling and sieving satisfied the morphological and structural features required for the re-manufacturing

* Corresponding author.
E-mail address: sonia.fiorilli@polito.it (S. Fiorilli).

https://doi.org/10.1016/j.ceramint.2024.06.206
Received 28 February 2024; Received in revised form 30 May 2024; Accepted 15 June 2024
Available online 15 June 2024
0272-8842/© 2024 The Authors. Published by Elsevier Ltd. This is an open access article under the CC BY-NC-ND license (http://creativecommons.org/licenses/by-nc-nd/4.0/).

of new fuel electrodes and could be used for the production of SOCs at an industrial scale. Specifically, half-SOCs (composed of NiO-3YSZ fuel support layer, NiO-8YSZ fuel functional layer and 8YSZ electrolyte) have been re-manufactured including 30 wt% of recycled materials in their support layer and benchmarked against SOCs composed of 100 wt% of virgin powders in their support layer.

2. Materials and methods

Scrap half-cells (provided by ELCOGEN) in their entirety were crushed into fragments and dry-milled in a 250 ml zirconia grinding bowl (FritschTM), provided with 6 zirconia grinding balls with 30 mm diameter, by use of a planetary mono mill (FritschTM, Pulverisette 6 Planetary Mono Mill). The materials were subjected to three subsequent milling and sieving (below 25 μm) steps: the first milling/sieving was carried out on the crushed half-cells, the second and third ones on the powders with size below 25 μm each recovered from the previous milling/sieving step. The recovery yield for each milling/sieving step was evaluated as the ratio between the mass of powders recovered after sieving to the mass of powders before milling. Each milling was carried out at 450 rpm, the first one for 10h and the subsequent two for 6h, while automatic sieving below 25 μm was carried out for 1h.

The obtained powders were fully characterized in terms of crystalline phases, specific surface area, and particle size distribution. X-Ray Diffraction (XRD, Panalytical, Xpert3 MRD) analysis was carried out using Cu Kα radiation at a voltage of 40 kV and a current of 40 mA, in the 2θ range of 10–70°. N_2 adsorption-desorption isotherm analyses were conducted by using an ASAP2020 Micromeritics analyser after degassing the powders at 150 °C for 4h, to evaluate their specific surface area (SSA). The Brunauer–Emmett–Teller (BET) equation was used to calculate the specific surface area (SSA_{BET}) in the 0.04–0.2 relative pressure range. A Zetasizer nano ZS90 (Malvern Instruments Ltd., Malvern, UK) was used at room-temperature (RT) to assess their average particle size distribution (PSD). Field Emission Scanning Electron Microscopy (FESEM, Jeol, JCM-6000Plus, Benchtop SEM) was performed in high vacuum conditions and at a voltage of 5 kV and 15 kV to evaluate the morphological features of the powders and the resulting re-manufactured cells, respectively.

Two sets of fuel cells were fabricated including 30 wt% of recovered powders in their tape-cast fuel support electrodes: button cells and large area cells. The viscosity of pastes for tape-casting was measured by use of a viscometer (Anton Paar ViscoQC 300) employing an RH4 spindle, at 30 rpm. Temperature control was carried out throughout the viscosity measurements by use of a Pt100 temperature sensor. Thin layers (i.e., fuel functional layer and electrolyte) were instead produced through a conventional screen-printing technology [7]. The sintering process for the half-cells was conducted at 1400 °C, as a result of various ramp rates. A first step was carried out at 50 °C h^{-1} to burn the binder, succeeded by a second step with a sintering rate of 100 °C h^{-1} up to the peak temperature of 1400 °C, with a dwelling time of 1 h. The cooling phase was also controlled, starting with a ramp rate of 100 °C h^{-1} down to 600 °C, and followed by a cooling rate of 300 °C h^{-1} until reaching room temperature. For full cells, the top air electrode was sintered at 950 °C for 1 h, with a heating rate of 100 °C h^{-1}. Full button cells with a diameter of 20 mm were electrochemically tested using an open-perimeter cell housing. Compressed air was supplied from the air electrode, while a mixture of dry H_2 and N_2 was provided from the fuel electrode side. Both the current-voltage (I–V) characteristics and electrochemical impedance spectroscopy (EIS) spectra were recorded. For the assessment of mechanical strength, instead, 50 × 50 mm^2 half-cells were subjected to testing in accordance with the ASTM C 1499-03 standard using ring-on-ring test equipment.

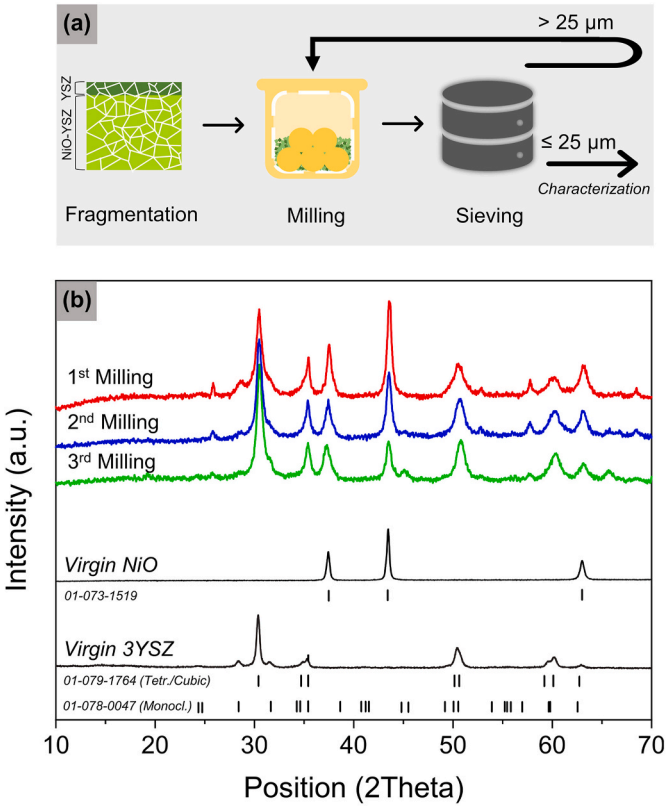


Fig. 1. Schematization of the multi-step milling/sieving process investigated for the recovery of NiO-YSZ powders from waste half-SOCs (a). XRD diffractograms show the crystalline phase evolution of the powders recovered after each step (b). Diffractograms of the virgin NiO and YSZ powders used for the manufacturing of standard SOCs are shown in the bottom part of the plot for comparison.

Table 1
Wt.% of NiO-YSZ powders sieved below 25 μm after each milling step, and corresponding specific surface area (m^2 g^{-1}) and average particle size (nm) values. The wt.% of powders with a size below 25 μm recovered after each step is also reported. For steps 2 and 3, the mass of powders subjected to milling corresponds to the fraction with a size below 25 μm recovered from the previous milling/sieving step, as detailed in section 2. The distribution of particle size is plotted and reported in the *Supplementary Information* section (Fig. S3) as a result of Dynamic Light Scattering analysis.

Milling step	Sieved powders ≤25 μm (wt.%)	Specific Surface Area (m^2 g^{-1})	Average Particle Size[a] (nm)
1 (10 h)	45	6	500 ± 140
2 (6h)	13	10	440 ± 110
3 (6h)	3	11	410 ± 100

[a] (derived from distribution % intensity).

3. Results and discussion

3.1. NiO-YSZ powders recovered from scrap half-cells

The considered scrap half-cells are constituted by an NiO fuel contact layer (5–10 μm), an NiO-3YSZ fuel support layer (380–390 μm), an NiO-8YSZ fuel functional layer (10–15 μm) and an 8YSZ electrolyte (3–6 μm). The received scrap half-cells were fragmented and milled in their entirety. The recovered powders will be hereafter referred to as NiO-YSZ composite powders, with the NiO-3YSZ component constituting 90 wt % of the milled material. 3YSZ presents a monoclinic and tetragonal crystal structure, while a tetragonal/cubic structure is associated with 8YSZ [8].

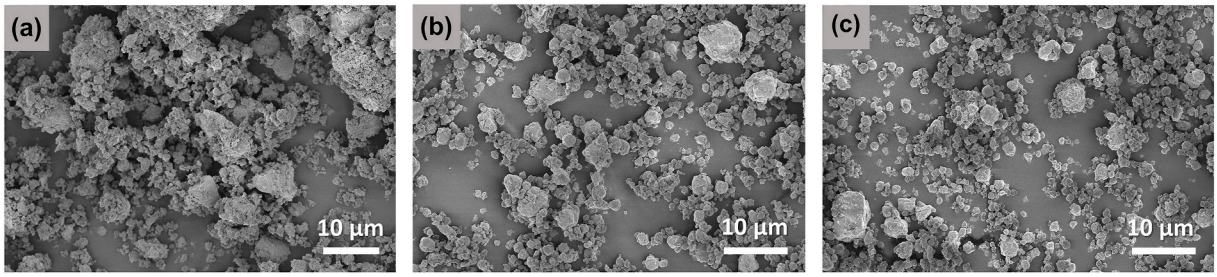


Fig. 2. FESEM micrographs of the NiO-YSZ powders recovered from waste half-SOCs after the first (a), second (b) and third (c) milling/sieving steps of the recovery process investigated and schematized in Fig. 1a.

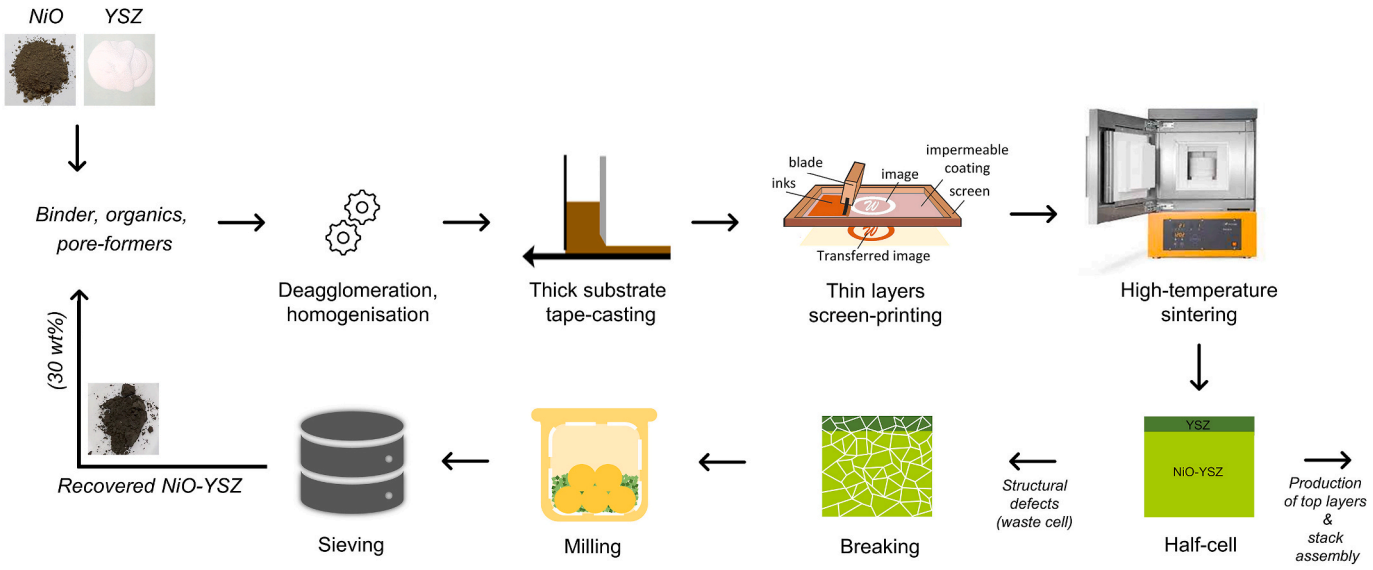


Fig. 3. Schematization of the manufacturing process of half-SOCs and of the recovery process of the ones presenting structural defects. Half-cells are constituted by an YSZ electrolyte, an NiO-YSZ fuel functional layer, an NiO-YSZ fuel layer support and an NiO fuel contact layer, and are inspected before depositing the upper protective layer and the air electrode.

XRD diffractograms (Fig. 1b) of NiO-YSZ composite powders after cell fragmentation and milling (Fig. 1a) demonstrated the overall preservation of both NiO and YSZ crystalline phases, without evidencing any progressive tetragonal-to-monoclinic transformation of YSZ because of exposing the powders to multiple milling steps and for prolonged times. The diffractograms of virgin NiO and 3YSZ are also provided as a reference.

As shown in Table 1, the recovery yield of powders with size below 25 μm significantly decreased from 45 wt% to 3 wt% from the first to the third step, respectively. Mass losses due to each milling step (i.e., the mass of powders not retrieved from the grinding balls and bowl) were constant, thus being negligible for step 1 and step 2 (0.4 and 0.9 wt%, respectively) and higher for step 3 (6.7 wt%). Therefore, the significant decrease of recovery yield at steps 2 and 3 could be ascribed to having reached, already after step 1, the maximum size reduction ratio achievable with the used processing conditions (i.e., number and size of grinding balls, bowl volume, and mass of powders detailed in section 2).

Concurrently to the decreased recovery yield, an increase in SSA and a decrease in PSD were observed from step 1 to step 3, ranging from 6 $m^2\ g^{-1}$ - 500 ± 140 nm to 11 $m^2\ g^{-1}$ and 400 ± 100 nm, respectively (Table 1). In particular, the most significant variations of SSA and PSD were observed between step 1 and step 2, from 6 $m^2\ g^{-1}$ to 500 ± 140 nm to 10 $m^2\ g^{-1}$ and 440 ± 110 nm, respectively. This was in good agreement with the relevant size reduction of large aggregates evidenced by FESEM analysis (Fig. 2) between the two steps.

For validation, the virgin NiO and 3YSZ powders used by ELCOGEN were analysed, giving average reference values of SSA and PSD equal to 8 $m^2\ g^{-1}$ and 550 ± 130 nm, respectively, as reported in Table S1 and Figs. S1 and S2 in the *Supplementary Information* section. As a result, the particle size and surface area of the recovered powders were well aligned to the target specifications already after the first processing step. Further milling/sieving steps were assessed as non-beneficial in terms of final features and recovery yield, and detrimental in terms of energy consumption at an industrial scale. A single 10 h-milling step, followed by sieving below 25 μm, was therefore selected for the recovery of the NiO-YSZ composite powders to be used for the re-manufacturing of SOCs fuel support layers containing 30 wt% of recovered material.

3.2. *Re-manufacturing and characterization of SOCs with 30 wt% of recovered material in their support layer*

After the recovery of powders, new cells were re-manufactured including 30 wt% of recovered material in their fuel support layer and compared to standard cells.

A schematization of the overall manufacturing (and re-manufacturing) process is illustrated in Fig. 3. Half-SOCs were produced through the tape-casting of the thick fuel support layer and the screen-printing of thin layers (i.e., fuel functional layer and electrolyte) [7] and were used for mechanical testing. For morphological and electrochemical characterization, full SOCs were produced by depositing the air electrode on the half-SOCs, according to the same screen-printing method.

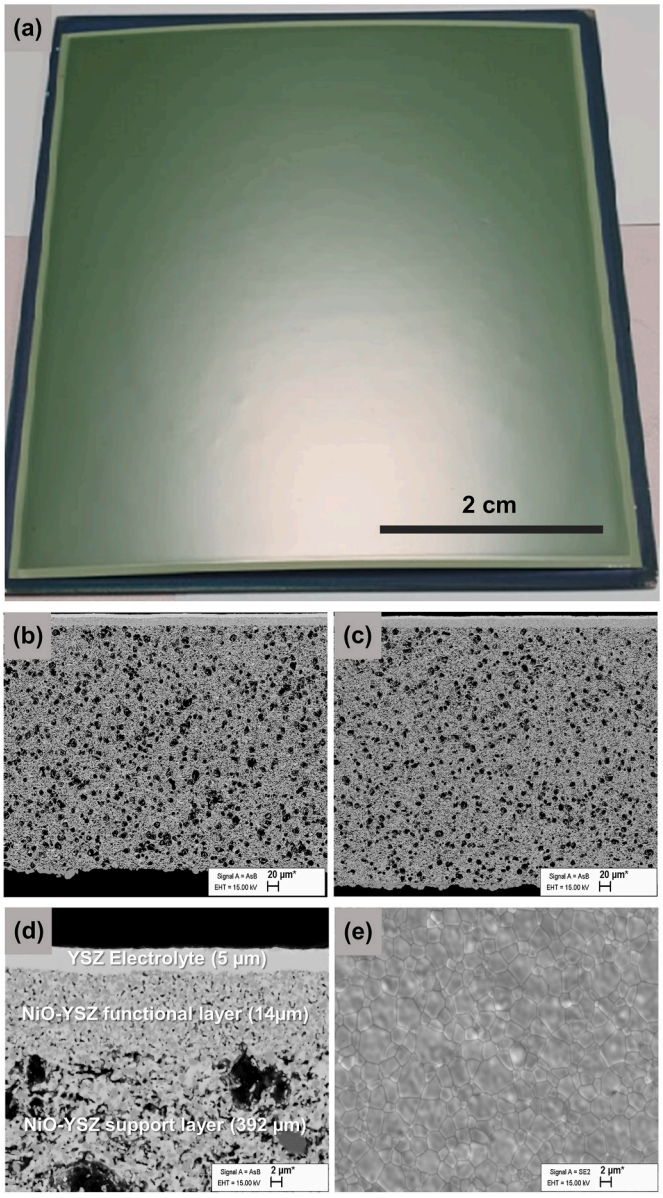


Fig. 4. Picture of a re-manufactured half-SOC containing 30 wt% of recycled NiO-YSZ powders (a). FESEM micrographs evidence the entire cross-section of a standard half-SOC (b) in comparison with a re-manufactured half-SOC (c). A higher magnification micrograph of the re-manufactured half-cell enables to distinguish the dense 8YSZ electrolyte from the low-porous NiO-8YSZ functional layer and the highly-porous NiO-3YSZ support layer containing recovered NiO-YSZ (d). The morphology of the 8YSZ electrolyte surface is also shown (e).

Standard half-cells consisted of a support layer made of NiO-3YSZ 50:50 by weight, a fuel functional layer made of NiO-8YSZ 50:50 by weight, and an 8YSZ electrolyte. Based on the powder weights of NiO, 3YSZ and 8YSZ standardly used for the manufacturing of half-cells, and considering that the re-manufactured support layers included 30 wt% of material recovered from half-scrap cells, the calculated NiO:3YSZ:8YSZ weight ratio in the re-manufactured support layers resulted as 49.7:49.0:1.3. The minimal fraction of fully-stabilized zirconia (8YSZ) was therefore not expected to significantly influence the overall functional properties of the re-manufactured cells.

To include the recovered powders in the support layer of these cells, a batch of slurry containing 30 wt% of recycled NiO-YSZ powder was prepared for tape-casting. Overall, the slurry showed a 25 % increase in viscosity compared to the standard formulation, resulting in a 20 % thicker tape-cast support layer. This was most likely attributed to the irregular shape [9,10], slight deviation of SSA and average particle size [11] and different surface chemistry shown by the recycled composite NiO-YSZ compared to the virgin NiO and YSZ powders used for standard manufacturing. A comparison between FESEM micrographs in Fig. 2 and Fig. S1 (Supplementary Information section) highlights the different surface morphology of recycled and virgin powders, respectively. Additionally, SSA and PSD values in Table 1 and Table S1 evidence the recovery of powders with slightly smaller average size with respect to the virgin powders, resulting in an increased paste viscosity.

Table 2
Comparison of the equiaxial flexural strengths of standard and re-manufactured SOCs.

Type of cell	Equiaxial strength (MPa)
Standard[a]	230 ± 14
Re-manufactured[b]	156 ± 21

[a] Average values derived from testing 5 standard cells.
[b] Average values derived from testing 7 re-manufactured cells.

Standard and re-manufactured (i.e., including 30 wt% of recovered material) fuel support layers were therefore produced through tape-casting. Half and complete SOCs were obtained from both types of substrates, according to the process described at the beginning of this section, and eventually characterized. A picture of a re-manufactured half-cell is shown in Fig. 4a, demonstrating a successful fabrication free from structural defects. From a microstructural cross-section analysis, the fuel support layer of a re-manufactured full cell (Fig. 4c) resulted very similar to that of a standard full cell (Fig. 4b) after sintering. No large agglomerates or other potentially detrimental inclusions, as well as cracks, were observed along its cross-section although containing 30 wt% of recycled material in the tape-cast fuel support layer. A higher magnification micrograph of the full re-manufactured cell (Fig. 4d) evidences the dense YSZ electrolyte, distinguishable from the low-porous functional layer and the highly porous fuel support layer including the recycled material. From a top-view micrograph of the cell (Fig. 4e), the electrolyte did not show any deformation or detachment from the lower cell components, yielding a continuous and well-adhered layer with good crystal grain cohesion after sintering.

In view of stack assembly, re-manufactured half-cells were mechanically tested to evaluate the influence of recycled materials on their overall strength. According to the results reported in Table 2, an average decrease from 230 MPa to 156 MPa was registered for the equiaxial strength, compared to standard cells.

This decrease may be ascribed to the reduced sintering activity of the recovered composite powders [12], which were already subjected to sintering, as well as to a possible deviation in terms of porosity and pore morphology [13,14] with respect to standard tape-cast fuel support electrodes. These average strength values resulted from testing 5 standard cells and 7 re-manufactured cells. This can be generally considered satisfactory for the evaluation of the mechanical strength of cells produced through a well-established industrial process. In this specific case, however, smaller cells were manufactured due to the limited amount of recycled NiO-YSZ material (ca. 300 g) compared to quantities generally processed at the industrial scale. Therefore, the resulting flexural strength tests could be considered as a comparative indication for this first re-manufacturing trial. Overall, the obtained values were lower compared to mechanical resistances reported in the literature [15]. Future works could focus on the careful optimization of the slurries containing NiO-YSZ particles, thus elucidating the effect of particle aggregation and slurry viscosities on the mechanical strength of the re-manufactured cells.

A complementary electrochemical cell evaluation was eventually performed (Fig. 5). According to the *j-V* curves shown in Fig. 5a and b,

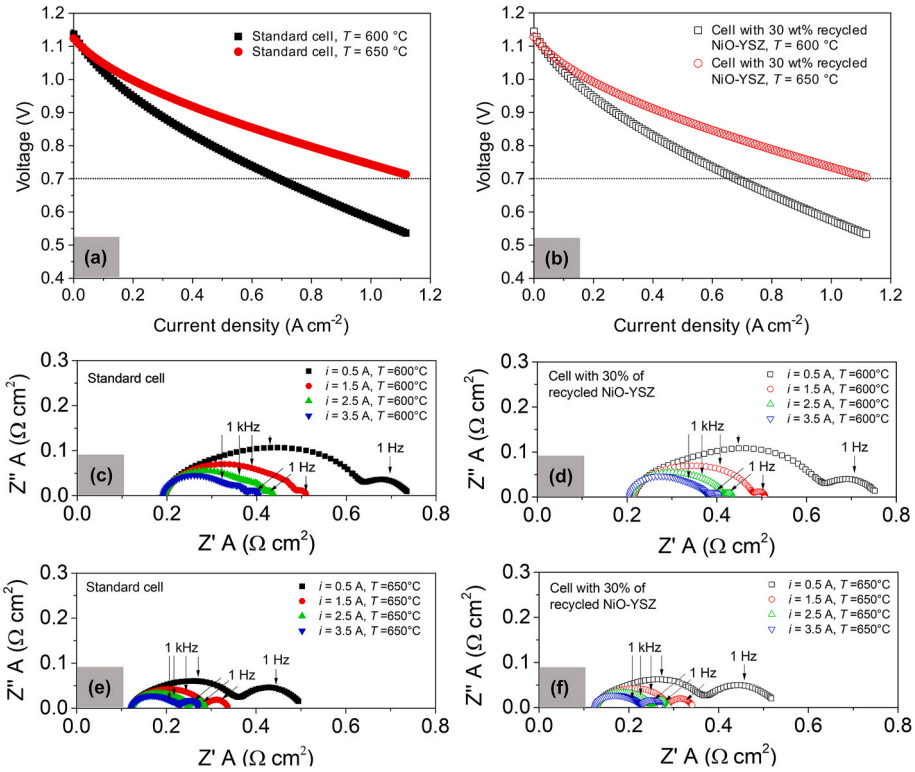


Fig. 5. Current-polarization curves of a standard SOC (a) and of a re-manufactured SOC containing 30 wt% of recovered material in its fuel electrode (b) at 600 and 650 °C. Nyquist plots showing the EIS measurements of a standard SOC and of a re-manufactured SOC at 600 and 650 °C with an applied current of 0.5, 1.5, 2.5 and 3.5 A (c, d, e, f). Both SOCs have been manufactured at ELCOGEN in the same way.

Table 3
R_s, R_{pol} and R_{tot} values (mΩ cm^2) for a standard SOC and for a re-manufactured SOC containing 30 wt% of recycled NiO-YSZ in its fuel support layer, at 600 °C and 650 °C and with an applied current density of 0.5 and 0.8 A cm^{-2}.

	Standard cell (mΩ cm^2)						Cell with 30 wt% of recycled powder (mΩ cm^2)					
	T = 600 °C			T = 650 °C			T = 600 °C			T = 650 °C		
	R_s	R_{pol}	R_{tot}	R_s	R_{pol}	R_{tot}	R_s	R_{pol}	R_{tot}	R_s	R_{pol}	R_{tot}
j ≈ 0.5 (A cm^{-2})	195.3	312.4	507.7	124.0	211.6	335.6	214.1	292.6	506.7	129.7	212.1	341.8
j ≈ 0.8 (A cm^{-2})	194.4	243.0	437.4	123.4	163.0	286.4	209.1	226.1	435.2	127.2	161.7	288.9

both standard and recycled cells measured current density values of 0.68 A cm^{-2} and 1.12 A cm^{-2} at 600 and 650 °C, respectively, showing an overall equivalent performance. Similarly, EIS measurements were carried out at 600 °C (Fig. 5c and d) and 650 °C (Fig. 5e and f). As shown in **Table 3**, similar serial and polarization resistance values were measured for both cells at these temperatures and with applied currents of 0.5 and 0.8 A cm^{-2}. At 0.5 A cm^{-2} and 600 °C, the standard cell presented an R_s equal to 195.3 mΩ cm^2 and an R_{pol} equal to 312.4 mΩ cm^2, while the cell with recycled material showed 214.2 mΩ cm^2 and 296.6 mΩ cm^2, respectively. These negligible differences of mΩ cm^2 can be due to the normal deviation that is observed in cells during the regular process fabrication or due to the fitting of the EIS spectra. One can notice from Table 3 that the % difference of the overall resistance R_{tot} of the cells at the different currents and temperature values is below 2 %. Overall, the serial resistance includes the ohmic resistance of the electrolyte and the current collection contributions [16]. Therefore, metallic Ni was able to provide a good percolation also in the fuel electrode of the re-manufactured cell, without affecting its diffusion properties during the reduction process.

4. Conclusions

A multi-step milling/sieving process was investigated for the recovery of NiO-YSZ composite powders from waste half-cells derived from SOC production. After a single 10 h-milling step followed by sieving below 25 μm, the powders reached the criteria required for the manufacturing of fuel support layers and could be directly re-used for this purpose. For the first time, re-manufactured SOCs containing 30 wt % of NiO-YSZ recovered material in their fuel support layer were fabricated. Despite showing a reduced equiaxial flexural strength, the electrochemical performances of re-manufactured SOCs were found to be equivalent to those of standard SOCs (containing 100 wt% of virgin materials) manufactured at an industrial scale, opening to a promising scenario for the future of SOC hydrogen technologies while also mitigating the risk of supply shortages for the growing demand of high-performing materials.

CRediT authorship contribution statement

Sofia Saffirio: Writing – review & editing, Writing – original draft, Visualization, Methodology, Investigation, Formal analysis, Data curation. **Simone Anelli:** Visualization, Formal analysis, Data curation.

Sergii Pylypko: Resources, Methodology, Investigation, Funding acquisition, Formal analysis, Conceptualization. **Manasa Kumar Rath:** Resources, Methodology, Investigation, Funding acquisition, Formal analysis, Conceptualization. **Federico Smeacetto:** Writing – review & editing, Validation, Project administration, Funding acquisition, Conceptualization. **Sonia Fiorilli:** Writing – review & editing, Validation, Supervision, Project administration, Funding acquisition, Conceptualization.

Declaration of competing interest

The authors declare that they have no known competing financial interests or personal relationships that could have appeared to influence the work reported in this paper.

Acknowledgements

This project has received funding from the Fuel Cells and Hydrogen 2 Joint Undertaking (now Clean Hydrogen Partnership) under Grant Agreement No 101007216. This Joint Undertaking receives support from the European Union's Horizon 2020 Research and Innovation program, Hydrogen Europe and Hydrogen Europe Research.

Appendix A. Supplementary data

Supplementary data to this article can be found online at https://doi.org/10.1016/j.ceramint.2024.06.206.

References

[1] Research Nester, Fuel Cell Market Size & Share, Global Forecast Report 2035. https://www.researchnester.com/reports/fuel-cell-market/3310.
[2] S. Sarner, A. Schreiber, N.H. Menzler, O. Guillon, Recycling strategies for solid oxide cells, Adv. Energy Mater. 12 (35) (2022) 2201805.
[3] S. Saffirio, et al., Hydrothermally-assisted recovery of Yttria-stabilized zirconia (YSZ) from end-of-life solid oxide cells, Sustain. Mater. Technol. 33 (2022) e00473.
[4] G.T. Yenesew, E. Quarez, A.L.G. La Salle, C. Nicollet, O. Joubert, Recycling and characterization of end-of-life solid oxide fuel/electrolyzer ceramic material cell components, Resour. Conserv. Recycl. 190 (2023) 106809.
[5] S. Sarner, N.H. Menzler, A. Hilgers, O. Guillon, Recycling and reuse strategies for ceramic components of solid oxide cells, ECS Trans. 111 (6) (2023) 1369.
[6] C. Kaiser, T. Buchwald, U.A. Peuker, Ultrasonic decoating as a new recycling path to separate oxygen side layers of solid oxide cells, Green Chem. 26 (2023) 960.
[7] J. Wang, D. Yan, J. Pu, B. Chi, L. Jian, Fabrication and performance evaluation of planar solid oxide fuel cell with large active reaction area, Int. J. Hydrogen Energy 36 (2011) 7234–7239.
[8] T. Götsch, W. Wallisch, M. Stöger-Pollach, B. Klötzer, S. Penner, From zirconia to yttria: sampling the YSZ phase diagram using sputter-deposited thin films, AIP Adv. 6 (2016) 25119.
[9] A. Bove, F. Calignano, M. Galati, L. Iuliano, Photopolymerization of ceramic resins by stereolithography process: a review, Appl. Sci. 12 (7) (2022).
[10] H.A. Barnes, A Handbook of Elementary Rheology, University of Wales, Institute of Non-Newtonian Fluid Mechanics, 2000.
[11] I.L. de Camargo, M.M. Morais, C.A. Fortulan, M.C. Branciforti, A review on the rheological behavior and formulations of ceramic suspensions for vat photopolymerization, Ceram. Int. 47 (9) (2021) 11906–11921.
[12] T. Matsushima, H. Ohrui, T. Hirai, Effects of sinterability of YSZ powder and NiO content on characteristics of Ni-YSZ cermets, Solid State Ionics 111 (1998), 315-231.
[13] S. Watanabe, S. Sukino, T. Miyasaka, K. Sato, K. Yashiro, T. Kawada, T. Hashida, Influences of Ni content and porosity on mechanical properties of Ni–YSZ composites under solid oxide fuel cell operating conditions, J. Mater. Sci. 55 (2020) 8679–8693.
[14] C.K. Ding, J.D. Zhang, Y.L. Liu, J.Y. Gou, J.P. Luan, Effects of pore-forming agent on characterization of NiO/YSZ porous anode for SOFC, Inside MS 848 (2016) 389–395.
[15] D.-W. Ni, B. Charlas, K. Kwok, T.T. Molla, P.V. Hendriksen, H.L. Frandsen, Influence of temperature and atmosphere on the strength and elastic modulus of solid oxide fuel cell anode supports, J. Power Sources 311 (2016) 1–12.
[16] S. Anelli, et al., Co-electrolysis of steam and carbon dioxide in large area solid oxide cells based on infiltrated mesoporous oxygen electrodes, J. Power Sources 478 (2020) 228774.